OPEN ACCESS
JOURNAL OF ADVANCED DIELECTRICS
Vol. 11, No. 5 (2021) 2160007 (10 pages)

DOI: 10.1142/S2010135X21600079

Specific features of SH-waves propagation in structures with prestressed inhomogeneous coating made of piezoceramics based on $LiNbO_3$

T. I. Belyankova*,‡, E. I. Vorovich†, V. V. Kalinchuk* and O. M. Tukodova†
*Department of Mechanics
Mathematics and Nanotechnology
Southern Scientific Center of RAS
41 Chekhov Avenue, 344006 Rostov-on-Don, Russia
†Department of Applied Mathematics
Don State Technical University
1 Gagarin Square, 344010 Rostov-on-Don, Russia
‡tbelen415@mail.ru

Received 14 April 2021; Accepted 19 May 2021; Published 21 June 2021

Within the framework of the linearized theory of electroelastic wave propagation, a model of a piezoelectric structure with a prestressed functionally graded coating made of piezoceramics of a trigonal system with a symmetry class of 3m is considered. The ferroelectric $LiNbO_3$ is used as the main material of the structure. The initial deformed state of the coating material is homogeneous, induced by the action of initial mechanical stresses and an external electrostatic field, the properties of the coating continuously change in thickness. By the example of the problem of the propagation of SH-waves from a remote source for structures with an inhomogeneous prestressed coating in the case of an electrically free and short-circuited surface, the influence of the nature and localization of the inhomogeneity of the coating on the features of SAW propagation is studied. The separate and combined effects of initial actions on changes in the physical properties of the structure, the transformation of the surface wave field, and the change in the SAW velocities in a wide frequency range is studied. The results obtained in this work are useful for understanding the dynamic processes in prestressed piezoelectric structures, in the optimization and design of new structures and devices on SAW with high performance characteristics.

Keywords: Piezoelectric structure; lithium niobate ($LiNbO_3$); functionally graded piezoelectric material (FGPM); surface acoustic waves (SAW); Bluestein–Gulyaev wave (WBG); initial deformed state (IDS).

1. Introduction

The foundations for the use of piezoactive materials for the creation of acoustoelectronic devices were laid in the 60–70s of the last century.[1–3] The area of application and the range of problems solved with the help of acoustoelectronic devices is determined by the velocity, characteristics of propagation and localization of (SAW).[4–6] The development of technologies for the production of artificial piezoelectric materials makes it possible to create a wide range of microelectromechanical systems (MEMS), sensors and actuators for various purposes, such as high-precision sensors, filters, converters, generators, power transmission devices, etc. The variety of problems solved using modern electronic and electromechanical systems, the need for an adequate assessment of the properties and performance of the structures used, depending on the operating conditions, necessitate the development of structural modeling using functionally graded components,[7–12] layers, shapes with various inclusions and coatings,[13–15] designs from synthetic bi- and multimaterials. The majority of piezoelectric ceramics (ferroelectric ceramic materials - FPM), commercially available in the world, are multicomponent systems of lead-containing complex oxides based on solid solutions of lead zirconate-titanate (PZT). In accordance with environmental requirements for these piezoceramics, it is necessary to exclude toxic lead oxide from the technological process and to find new piezoelectric materials that are not inferior in properties to PZT ceramics. Long-term experience in the development of highly efficient FPMs makes it possible to obtain a group of lead-free materials based on alkali metal niobates - lithium and sodium, which have a number of unique properties that are not realized in PZT compositions.[16–20]

The advantages of such FPMs are as follows:

— high velocity of sound, which determines the high-frequency (HF) range of operation of the transducer, as well as the ability to obtain a given frequency on less thin plates, which simplifies the manufacturing technology of HF devices due to the possibility of increasing their

‡Corresponding author.

resonant dimensions, which, in turn, is beneficial from the point in terms of reducing the capacity of the converter;
— low density, leading, on the one hand, to a significant reduction in the weight of products, and on the other, to a decrease in acoustic impedance;
— very low dielectric constant, which is important for electrical matching with the generator and load;
— increased thickness coefficient of electromechanical connection;
— sufficient anisotropy of piezoelectric properties, which allows improving the signal-to-noise ratio and simplifying the production technology, excluding the operation of cutting the material;
— low dielectric and moderate mechanical losses, which is important for obtaining short pulses and uniform amplitude-frequency characteristics.

The crystal structure, electro physical and thermal properties of the solid solution $Na_{0.875}Li_{0.125}NbO_3$, modified with strontium and other elements,[18] were studied in a wide range of temperatures and frequencies of an alternating electric field. The effects of low-frequency dispersion of the dielectric constant, caused by the influence of electrical conductivity, are revealed. The dielectric properties of solid solutions of binary systems based on sodium–potassium and sodium–lithium niobates were studied in a wide range of external influences[19]: temperature 25°C–750°C, alternating frequency 25 Hz–10^6 Hz and constant electric field strength up to 30 kV/cm. The features of the microstructure and elastic properties of ceramic solid solutions $Li_xNa_{1-x}Ta_yNb_{1-y}O_3$, depending on the composition and synthesis temperature, were studied for the first time.[20] A specific feature of the change in the mechanical properties of $Li_{0.17}Na_{0.83}Ta_yNb_{1-y}O_3$ solid solutions depending on the parameters of the technological process is shown. The complexity of modeling functional-gradient materials (FGM) lies in the impossibility of obtaining a rigorous analytical solution, which leads to the need to simplify the model. It is often assumed that the properties of a material change with the same intensity according to the same law and one spatial variable. Such assumptions make it possible to obtain an analytical solution, but to study the heterogeneity of the properties of materials, their use is effective only in certain special cases. When modeling FGM, various approaches are used: division into layered elements with linear or quadratic changes in properties; as functional dependencies, either power series expansions or easily differentiable functions and polynomials are used. When modeling bi- and multimaterials, as a rule, numerical methods are used. To study the propagation of surface waves in prestressed piezoelectric structures, a generalized model of a homogeneous half-space with an inhomogeneous layer of a functionally graded piezoelectric material (FGPM) is proposed.[21–26] Boundary and mixed dynamic problems of electroelasticity are considered, the solution of which is presented in Fourier transforms. A combination of an analytical solution for a homogeneous half-space with a numerical reconstruction of the solution for an inhomogeneous layer is used. Within the framework of the proposed model, the influence of the nature, the area of localization and the intensity of changes in various physical parameters of inhomogeneity on the propagation of surfactants with monotonic and nonmonotonic changes in the properties of coatings from FGPM is investigated. The development of the model is associated with the complication of the coverage, which is modeled either by an FGPM layer, or by a package of both homogeneous and heterogeneous layers.[21–26] The features of the propagation of surfactants and the coefficient of electromechanical coupling in piezoelectric structures with a functionally graded coating, the properties of which change in a piecewise-continuous manner, have been investigated in detail.[22–25] The influence on the distribution of SAW, characteristics, localization, intensity of change of various physical modules relative to one reference material was studied. The proposed model is improved for the study of heterogeneous coatings of two or more piezoelectric materials.[24–26] The regularities of the influence of the combination of the properties of coating materials and the localization of inhomogeneity on the features of the propagation of surface shear horizontally polarized waves have been established. In this paper, we consider a piezoelectric structure consisting of a homogeneous half-space with a prestressed functionally graded coating, the properties of which vary throughout the thickness in a continuous nonmonotonic manner. For problems with an electrically open or closed free surface, the influence of the gradient of changes in the elastic, piezoelectric and dielectric properties of the coating material and the localization of inhomogeneity on the SAW velocities in a wide frequency range were investigated. The features of the effect of the initial mechanical and electrical actions on the change in the properties of a functionally graded coating made of a piezoelectric material of a trigonal system with a symmetry class of 3m were investigated. The results of calculating the SAW velocities depending on the type and magnitude of the initial actions for structures with different types of inhomogeneity were presented.

2. Statement of the Problem

We consider the problem of propagation in the direction x_1 of SH-waves over the surface of a composite piezoactive medium, which is a homogeneous half-space $x_2 \le 0$, $|x_1|, |x_3| \le \infty$ with a coating $0 < x_2 \le H$ (Fig. 1).

The coating is made of a functionally graded piezoelectric material (FGPM), the properties of which are continuously changing in thickness:

$$\begin{aligned} \rho^{(1)} &= \rho_0 f_\rho^{(1)}(x_2), \quad c_{ij}^{(1)} = c_{ij}^0 f_c^{(1)}(x_2), \\ e_{ij}^{(1)} &= e_{ij}^0 f_e^{(1)}(x_2), \quad \varepsilon_{ij}^{(1)} = \varepsilon_{ij}^0 f_\varepsilon^{(1)}(x_2) \end{aligned} \tag{1}$$

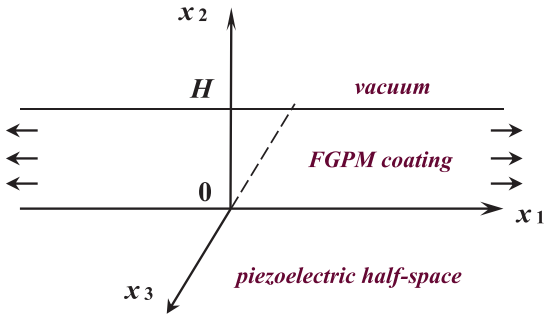

Fig. 1. Scheme of the problem.

$\rho_0, c_{ij}^0, e_{ij}^0, \varepsilon_{ij}^0$-respectively, the density and elastic, piezoelectric and dielectric modules of the half-space material, for which $LiNbO_3$ is used — a piezoelectric of the 3m class with the symmetry axis directed along the axis x_3, the polarization vectors of the half-space and the coating coincide. The IDS of the coating is homogeneous and is induced due to the action of the initial mechanical stresses and a homogeneous electrostatic field:[21,23,25,26]

$$\mathbf{R} = \mathbf{r}\cdot\Lambda, \quad \mathbf{G} = \Lambda\cdot\Lambda^{\mathbf{T}}, \quad \Lambda = \begin{pmatrix} v_1 & 0 & 0 \\ 0 & v_2 & 0 \\ 0 & 0 & v_3 \end{pmatrix}, \quad (2)$$
$$\varphi_0 = -\mathbf{E}_0\cdot\mathbf{R}, \quad v_i = \text{const}$$

Here $\mathbf{R}, \mathbf{r}$ are the radius vectors of the point of the medium in the IDS and the natural state (NS), respectively, $v_i = 1+\delta_i, \delta_i$ are the main relative elongations, φ_0 is the electric potential, $\mathbf{E}_0$ is the intensity of the electric field in the IDS.

Harmonic steady vibrations of the medium are caused by the action of a remote source, the dynamic process satisfies the conditions ($k = 3,4, n = 1,2$)

$$u_1^{(n)} = u_2^{(n)} = 0, \quad \partial/\partial x_3 = 0, \quad u_k^{(n)} = u_k^{(n)}(x_1, x_2), \quad (3)$$

The problem of the propagation of SAW in a composite prestressed electroelastic medium is described by the equations ($\Theta^{(1)} = \mathbf{\Pi}^{(1)} + \mathbf{m}^{(1)}$):[21,26]

$$\nabla_0\cdot\Theta^{(n)} = \rho_0^{(n)}\ddot{\mathbf{u}}^{\mathbf{e}(n)}, \quad \nabla_0\cdot\mathbf{d}^{(n)} = 0. \quad (4)$$

The equation for vacuum has the form

$$\Delta\varphi^{(0)} = 0. \quad (5)$$

The boundary conditions are as follows:

on a surface $x_2 = H$:

absence of mechanical stresses

$$\mathbf{n}\cdot\Theta^{(1)} = 0, \quad (6)$$

electrically "open" case

$$\mathbf{n}\cdot\mathbf{d}^{(1)} = \mathbf{n}\cdot\mathbf{d}^{(0)}, \quad \varphi^{(1)} = \varphi^{(0)} \quad (7)$$

or electrically "short" case

$$\varphi^{(1)} = 0, \quad (8)$$

on a surface $x_2 = 0$

continuity of mechanical and electrical characteristics of the layer and half-space

$$\mathbf{u}^{\mathbf{e}^{(1)}} = \mathbf{u}^{\mathbf{e}^{(2)}}, \quad \mathbf{n}\cdot\Theta^{(1)} = \mathbf{n}\cdot\Theta^{(2)}, \quad \varphi^{(1)} = \varphi^{(2)}, \quad \mathbf{n}\cdot\mathbf{d}^{(1)} = \mathbf{n}\cdot\mathbf{d}^{(2)} \quad (9)$$

damping of oscillations at infinity

$$\mathbf{u}^{\mathbf{e}^{(2)}}|_{x_2\to-\infty} \to 0, \quad \varphi^{(0)}|_{x_3\to\infty} \to 0. \quad (10)$$

Here ∇_0 is the Hamilton operator, $\mathbf{u}^{\mathbf{e}^{(n)}} = \{u_3^{(n)}, u_4^{(n)} = \varphi^{(n)}\}$ is the extended displacement vector, $\varphi^{(n)}$ is the electric potential, $\mathbf{n}$ is the vector of the outer normal to the surface of the structure in the coordinate system associated with the NS; $\rho_0^{(n)}$ - material density n - component of structure in NS ($n = 1, 2$ - coating and half-space); Δ - Laplace operator. The components of the linearized tensor Piola $\mathbf{\Pi}^{(n)}$, Piola–Maxwell stress tensors $\mathbf{m}^{(n)}$ and the "material" induction vector $\mathbf{d}^{(n)}$ are represented as ($k, l, s, p = 1,2,3, n = 1,2$):[21,26]

$$\Theta_{lk}^{(n)} = \Pi_{lk}^{(n)} + m_{lk}^{(n)}, \quad \Pi_{lk}^{(n)} = c_{lksp}^{(n)*}u_{s,p}^{(n)} + e_{lkp}^{(n)*}\varphi_{,p}^{(n)},$$
$$m_{lk}^{(n)} = \zeta_{lksp}^{(n)*}u_{s,p}^{(n)} + \psi_{lkp}^{(n)*}\varphi_{,p}^{(n)}, \quad (11)$$
$$d_l^{(n)} = g_{lsp}^{(n)*}u_{s,p}^{(n)} - \eta_{lp}^{(n)*}\varphi_{,p}^{(n)}$$

Further, for convenience of presentation, we use a more compact representation of the stress tensor and the induction vector

$$\Theta_{lk}^{(n)} = \theta_{lksp}^{(n)}u_{s,p}^{(n)} + \theta_{lk4p}^{(n)}\varphi_{,p}^{(n)},$$
$$d_l^{(n)} = \theta_{l4sp}^{(n)}u_{s,p}^{(n)} + \theta_{l44p}^{(n)}\varphi_{,p}^{(n)} \quad (12)$$

with denotation ($k, l, s, p = 1,2,3$)

$$\theta_{lksp}^{(n)} = c_{lksp}^{(n)*} + M_{lksp}^{(n)}, \quad \theta_{lk4p}^{(n)} = e_{lkp}^{(n)*} + M_{lk4p}^{(n)}$$
$$\theta_{l4sp}^{(n)} = e_{lsp}^{(n)*} + M_{l4sp}^{(n)}, \quad \theta_{l44p}^{(n)} = -\eta_{lp}^{(n)*} \quad (13)$$
$$M_{lksp}^{(n)} = \zeta_{lksp}^{(n)*}, \quad M_{lk4p}^{(n)} = \psi_{lkp}^{(n)*}, \quad M_{l4sp}^{(n)} = \psi_{lsp}^{(n)*}.$$

The form of the coefficients $c_{lksp}^{(1)*}, e_{lsp}^{(1)*}, \zeta_{lksp}^{(1)*}, \psi_{lkp}^{(1)*}, \eta_{lp}^{(1)*}$ and $g_{lsp}^{(1)*} = e_{lsp}^{(1)*} + \psi_{lsp}^{(1)*}$ for the general case of prestressed coating is given in Refs. 21 and 26. It should be noted that the coefficients $c_{lksp}^{(1)*}$, $e_{lsp}^{(1)*}$ and $\eta_{lp}^{(1)*}$ are functions of x_2; the components $M_{lksp}^{(1)}$ do not depend of x_2 and are determined by the direction and magnitude of the intensity of the initial electrostatic field; components $\theta_{lksp}^{(1)}$ and $M_{lksp}^{(1)}$ depend on the nature and magnitude of the induced initial deformations. For a homogeneous substrate material in the NS, the following relations are executed:

$$c_{lksp}^{(2)*} = c_{lksp}^{(2)}, \quad e_{lsp}^{(2)*} = g_{lsp}^{(2)*} = e_{lsp}^{(2)},$$
$$\eta_{lp}^{(2)*} = \varepsilon_{lp}^{(2)}, \quad M_{lksp}^{(2)} = 0.$$

Within the framework of assumptions (1)–(3), problem (4)–(10) on vibrations of a composite electroelastic medium with a prestressed inhomogeneous coating has the form:[21–26]

for inhomogeneous coating $0 < x_2 \le H$

$$\sum_{k=1}^{2}[\theta_{k33k}^{(1)}u_{3,kk}^{(1)} + \theta_{k34k}^{(1)}u_{4,kk}^{(1)}] + \sum_{k=3}^{4}\theta_{23k2,2}^{(1)}u_{k,2}^{(1)} = \rho_0^{(1)}\frac{\partial^2 u_3^{(1)}}{\partial t^2}$$
$$\sum_{k=1}^{2}[\theta_{k43k}^{(1)}u_{3,kk}^{(1)} + \theta_{k44k}^{(1)}u_{4,kk}^{(1)}] + \sum_{k=3}^{4}\theta_{24k2,2}^{(1)}u_{k,2}^{(1)} = 0 \quad (14)$$

for substrate $x_2 \le 0$

$$\sum_{k=1}^{2}[\theta_{k33k}^{(2)}u_{3,kk}^{(2)} + \theta_{k34k}^{(2)}u_{4,kk}^{(2)}] = \rho_0^{(2)}\frac{\partial^2 u_3^{(2)}}{\partial t^2}$$
$$\sum_{k=1}^{2}[\theta_{k43k}^{(2)}u_{3,kk}^{(2)} + \theta_{k44k}^{(2)}u_{4,kk}^{(2)}] = 0 \quad (15)$$

For vacuum $x_2 > H$

$$\sum_{k=1}^{2}u_{4,kk}^{(0)} = 0. \quad (16)$$

The boundary conditions are represented as follows:

$x_2 = H$

$$\Theta_{23}^{(1)} = \sum_{k=3}^{4}[\theta_{23k2}^{(1)}u_{k,2}^{(1)}] = 0 \quad (17)$$

$$d_2^{(1)} = \sum_{k=3}^{4}[\theta_{24k2}^{(1)}u_{k,2}^{(1)}] = d_2^{(0)}, \quad u_4^{(1)} = u_4^{(0)} \quad (18)$$

$$u_4^{(1)} = 0 \quad (19)$$

$x_2 = 0$

$$\mathbf{u}^{e(1)} = \mathbf{u}^{e(2)}, \quad \Theta_{23}^{(1)} = \Theta_{23}^{(2)},$$
$$\varphi^{(1)} = \varphi^{(2)}, \quad d_2^{(1)} = d_2^{(2)} \quad (20)$$

$$x_2 \to -\infty : \mathbf{u}^{e(2)} \to 0, \quad x_2 \to \infty : u_4^{(0)} \to 0. \quad (21)$$

Taking into account the properties of the material and conditions (2), the coefficients $\theta_{lksp}^{(n)}$ in relations (14)–(21) take the form

$$\theta_{1331}^{(1)} = c_{44}^{(1)}v_3^2 + P_{11} - \varepsilon_0\frac{v_2v_3}{v_1}E_3^2,$$
$$\theta_{2332}^{(1)} = c_{44}^{(1)}v_3^2 + P_{22} - \varepsilon_0\frac{v_1v_3}{v_2}E_3^2,$$
$$\theta_{1341}^{(1)} = \theta_{1431}^{(1)} = e_{15}^{(1)}v_3 - \varepsilon_0\frac{v_2v_3}{v_1}E_3,$$
$$\theta_{2342}^{(1)} = \theta_{2432}^{(1)} = e_{15}^{(1)}v_3 - \varepsilon_0\frac{v_1v_3}{v_2}E_3,$$
$$\theta_{1441}^{(1)} = -\varepsilon_0\frac{v_2v_3}{v_1} - \beta_{11}^{(1)}, \quad \theta_{2442}^{(1)} = -\varepsilon_0\frac{v_1v_3}{v_2} - \beta_{11}^{(1)},$$
$$\beta_{kn}^{(1)} = \varepsilon_{kn}^{(1)} - \varepsilon_0\delta_{kn}, \quad E_k = v_k^{-1}W_k$$

here P_{ij} are the components of the Kirchhoff initial stress tensor[6–8]; δ_{kn}- Kronecker symbol.

Further, the dimensionless parameters are used[21–26]: $l' = l/H$, $\rho'^{(n)} = \rho^{(n)}/\rho^{(2)}$, $c_{ij}'^{(n)} = c_{ij}^{(n)}/c_{44}^{(2)}$, $e_{ij}'^{(n)} = e_{ij}^{(n)}\xi/c_{44}^{(2)}$, $\varepsilon_{ij}'^{(n)} = \varepsilon_{ij}^{(n)}\varepsilon^{(0)}\xi^2/c_{44}^{(2)}$, $\varphi'^{(n)} = \varphi^{(n)}/(\xi H)$, $E_k' = E_k/\xi$, $\xi = 10^{10}$ V/m; $\varepsilon^{(0)} = \varepsilon_0$ — dielectric constant of vacuum; $\kappa_2 = \omega h/V_S^{(2)}$ and $\kappa_{2e} = \omega h/V_{Se}^{(2)}$ — dimensionless frequencies, $V_{Se}^{(2)} = \sqrt{(c_{44}^{(2)} + (e_{15}^{(2)})^2/\varepsilon_{11}^{(2)})/\rho^{(2)}}$ and $V_S^{(2)} = \sqrt{c_{44}^{(2)}/\rho^{(2)}}$ — velocity of bulk shear waves with and without piezoelectric properties. Further strokes are omitted.

Next, we consider two problems:

problem I — "open case" is described by Eqs. (14)–(16) with the boundary conditions (17), (18), (20) and (21);

problem II — "short case" is described by Eqs. (14), (15) with the boundary conditions (17), (19)–(21).

3. Dispersion Equations of Problems

The solution of ***problems I and II*** is generated using the Fourier transform (α- the transformation parameter by coordinate x_1; $p = 3, 4$):[21–25]

$$U_p^{(1)}(\alpha, x_2) = \sum_{k=1}^{4}c_k^{(1)}y_{kp}^{(1)}(\alpha, x_2), \quad (22)$$

$$U_p^{(2)}(\alpha, x_2) = \sum_{k=1}^{2}f_{pk}^{(2)}c_k^{(2)}e^{\sigma_k^{(2)}x_2},$$
$$U_4^{(0)}(\alpha, x_2) = c_1^{(0)}e^{-\alpha x_2}. \quad (23)$$

Parameters $\sigma_k^{(2)}$ and coefficients $f_{pk}^{(2)}$ are given in Refs. 21–25. The functions $y_{kp}^{(1)}(\alpha, x_2)$ in expression (22) are linearly independent solutions of the Cauchy problem with the initial conditions $y_{kp}^{(1)}(\alpha, 0) = \delta_{kp}$ for the equation

$$\mathbf{Y}^{(1)\prime} = \mathbf{M}^{(1)}(\alpha, x_2)\mathbf{Y}^{(1)},$$
$$\mathbf{Y}^{(1)} = \begin{pmatrix}\mathbf{Y}_{\Sigma}^{1}\\ \mathbf{Y}_{\mathbf{u}}^{1}\end{pmatrix}, \quad \mathbf{Y}_{\Sigma}^{1} = \begin{Vmatrix}\Theta_{23}^{F(1)}\\ D_2^{F(1)}\end{Vmatrix},$$
$$\mathbf{Y}_{\mathbf{u}}^{1} = \begin{Vmatrix}U_3^{(1)}\\ U_4^{(1)}\end{Vmatrix}. \quad (24)$$

Here $\Theta_{23}^{F(n)}, D_2^{F(n)}, U_k^{(n)}$ — are the Fourier transforms of the component of the stress tensor, induction vector, and the extended displacement vector. The view of matrix $\mathbf{M}^{(1)}(\alpha, x_2)$ is given in Refs. 24–26. Unknown coefficients $c_k^{(n)}$

in representations (22), (23) are determined when boundary conditions are satisfied. The solution of system (20) is constructed numerically; a modification of the Runge–Kutta method is used in the work.

The dispersion equations of ***problems I*** and ***II*** for a piezoelectric structure with a functionally graded coating have the form:[23–26]

$$\det \mathbf{A} = 0. \tag{25}$$

Matrix $\mathbf{A}$ for ***problem I*** has the form

$$\mathbf{A^I} = \begin{vmatrix} y_{11}^{(1)} & y_{12}^{(1)} & y_{13}^{(1)} & y_{14}^{(1)} & 0 & 0 & 0 \\ \gamma y_{21}^{(1)} & \gamma y_{22}^{(1)} & \gamma y_{23}^{(1)} & \gamma y_{24}^{(1)} & 0 & 0 & -\varepsilon_0\alpha \\ \gamma y_{41}^{(1)} & \gamma y_{42}^{(1)} & \gamma y_{43}^{(1)} & \gamma y_{44}^{(1)} & 0 & 0 & -1 \\ 1 & 0 & 0 & 0 & -l_{11}^{(2)} & -l_{12}^{(2)} & 0 \\ 0 & 1 & 0 & 0 & 0 & -l_{22}^{(2)} & 0 \\ 0 & 0 & 1 & 0 & -1 & 0 & 0 \\ 0 & 0 & 0 & 1 & -f_{41}^{(2)} & -1 & 0 \end{vmatrix}, \tag{26}$$

Matrix $\mathbf{A}$ for ***problem II*** has the form

$$\mathbf{A^{II}} = \begin{vmatrix} y_{11}^{(1)} & y_{12}^{(1)} & y_{13}^{(1)} & y_{14}^{(1)} & 0 & 0 \\ y_{41}^{(1)} & y_{42}^{(1)} & y_{43}^{(1)} & y_{44}^{(1)} & 0 & 0 \\ 1 & 0 & 0 & 0 & -l_{11}^{(2)} & -l_{12}^{(2)} \\ 0 & 1 & 0 & 0 & 0 & -l_{22}^{(2)} \\ 0 & 0 & 1 & 0 & -1 & 0 \\ 0 & 0 & 0 & 1 & -f_{41}^{(2)} & -1 \end{vmatrix}, \tag{27}$$

where

$$l_{11}^{(2)} = c_{44}^{(2)}(1+\eta)\sigma_1^{(2)}, \quad l_{12}^{(2)} = e_{15}^{(2)}\sigma_2^{(2)}, \quad l_{21}^{(2)} = 0,$$
$$l_{22}^{(2)} = -\varepsilon_{11}^{(2)}\sigma_2^{(2)}, \quad f_{41}^{(2)} = \frac{e_{15}^{(2)}}{\varepsilon_{11}^{(2)}}, \quad \eta = \frac{(e_{15}^{(2)})^2}{\varepsilon_{11}^{(2)} c_{44}^{(2)}}, \quad \gamma = e^{\alpha H}.$$

4. Numerical Analysis

In this paper, piezoelectric structures made of ceramics based on $LiNbO_3$ with parameters are considered:[27,28]

$$\rho = 4.7 \cdot 10^3\,\mathrm{kg/m^3}, \quad c_{11} = 20.3 \cdot 10^{10}\,\mathrm{N/m^2},$$
$$c_{12} = 5.3 \cdot 10^{10}\,\mathrm{N/m^2}, \quad c_{13} = 7.5 \cdot 10^{10}\,\mathrm{N/m^2},$$
$$c_{14} = 0.9 \cdot 10^{10}\,\mathrm{N/m^2}, \quad c_{33} = 24.5 \cdot 10^{10}\,\mathrm{N/m^2},$$
$$c_{44} = 3 \cdot 10^{10}\,\mathrm{N/m^2}, \quad e_{15} = 3.7\,\mathrm{C/m^2},$$
$$e_{22} = 2.5\,\mathrm{C/m^2}, \quad e_{31} = 0.2\,\mathrm{C/m^2}, \quad e_{33} = 1.3\,\mathrm{C/m^2},$$
$$\varepsilon_{11}/\varepsilon_0 = 44, \quad \varepsilon_{33}/\varepsilon_0 = 29, \quad \varepsilon_0 = 8.85 \cdot 10^{-12}\,\mathrm{F/m}.$$

It is assumed that the coating of the structure is made of a functionally graded material, the properties of which vary in thickness as follows:[23–25]

$$f_s^{(1)}(x_2) = g_s^1 + g_s^2 f(x_2),$$

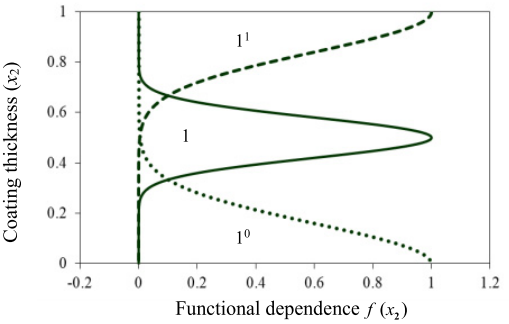

Fig. 2. The laws of changing the properties of the coating.

where, g_s^1, g_s^2, $(s = \rho, c, e, \varepsilon)$- are determined by the ratio of the modules of the main material and materials of inclusions; $f(x_2)$- determines the nature of the change in parameters over the thickness of the coating, the localization of changes and the size of the transition zone of one material into another (Fig. 2). In Fig. 2, solid (curve 1), dashed (curve 1^1) and dashed (curve 1^0) lines mark the curves of changes in properties when the heterogeneity is localized in the middle, at the surface, and at the base of the coating.

The gradient coefficients of changes in the properties of the coating are determined by the formulas

$$\gamma_s = r_s^{(1)}/r_s^{(2)}, \quad r_c^{(n)} = c_{44}^{(2)}, \quad r_e^{(n)} = e_{15}^{(2)}, \quad r_\varepsilon^{(n)} = \varepsilon_{11}^{(2)}.$$

The paper considers the separate and combined effect of the gradient coefficients of changes in the elastic, piezoelectric and dielectric properties of the SAW velocity material in the short and open case. The influence of the initial mechanical and electrical influences is shown on the example of a structure with a two-component $(m_1/m_s, s = 2, 3, 4)$ coating. In the materials of inclusions, the gradient coefficients of the parameter change were chosen from the condition $V_{Se}^{m_2} > V_{Se}^{m_3} > V_{Se}^{m_1} > V_{Se}^{m_4}$.

4.1. *Influence of the gradient coefficient of changes coating properties on the SAW velocity*

Figures 3–7 show the transformation of the relative velocities of the SAW ($V_F^{I,II}/V_{Se}^{(2)}$, where $V_F^{I,II} = \kappa_2/\xi$, ξ is the solution of Eq. (25) with notations (26) for problem for ***problem I*** and (27) for ***problem II***) depending on the change in the properties of the coating material in the short (Figs. 3–6) and open case (Fig. 7). In Figs. 3(b) and 4(b) for clarity of representation of the behavior of SAW velocities in case $\gamma_c = 0.6$ (curves 5), the first and second modes of surface waves are marked by dashed and dotted lines. Figure 3 shows the effect of changes in elastic modules ($\gamma_c, \gamma_e = \gamma_\varepsilon = 1$) on SAW velocity at localization of heterogeneity at the surface (Fig. 3(a)), in the middle (Fig. 3(b)) and at the base of the coating (Fig. 3(c)). The numbers 1–6 mark the curves corresponding to the values $\gamma_c = 2$, 1.8, 1.5, 0.8, 0.6, 0.4.

Figure 4 illustrates the effect of piezoelectric modules ($\gamma_e, \gamma_c = \gamma_\varepsilon = 1$) on the SAW velocity at localization of

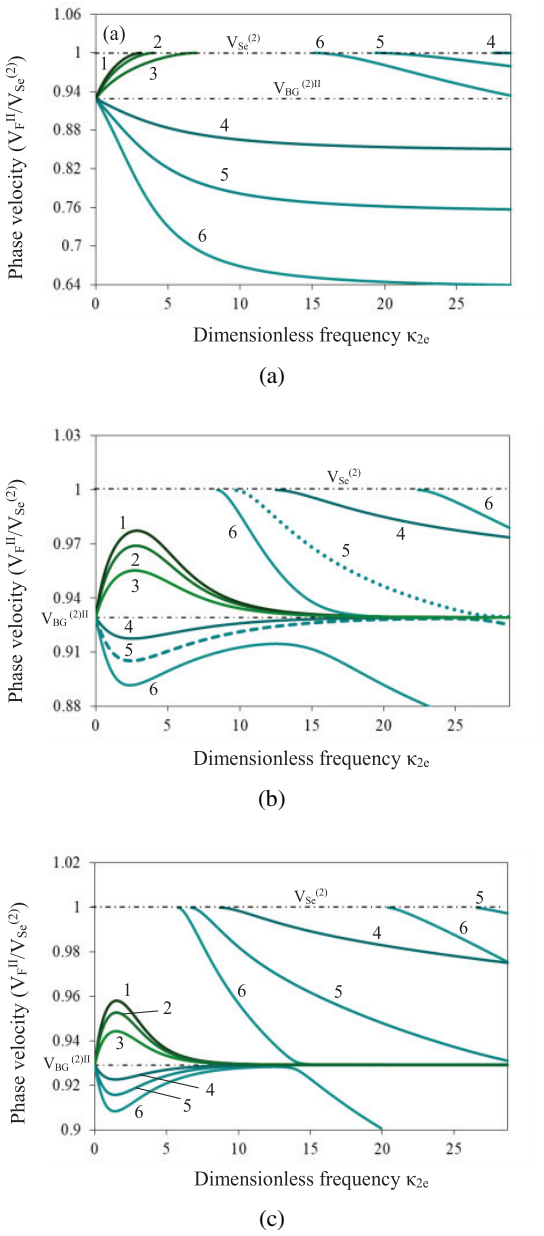

Fig. 3. Influence of the gradient coefficient of changes in the elastic properties of the coating on the SAW velocity at different localization of heterogeneity.

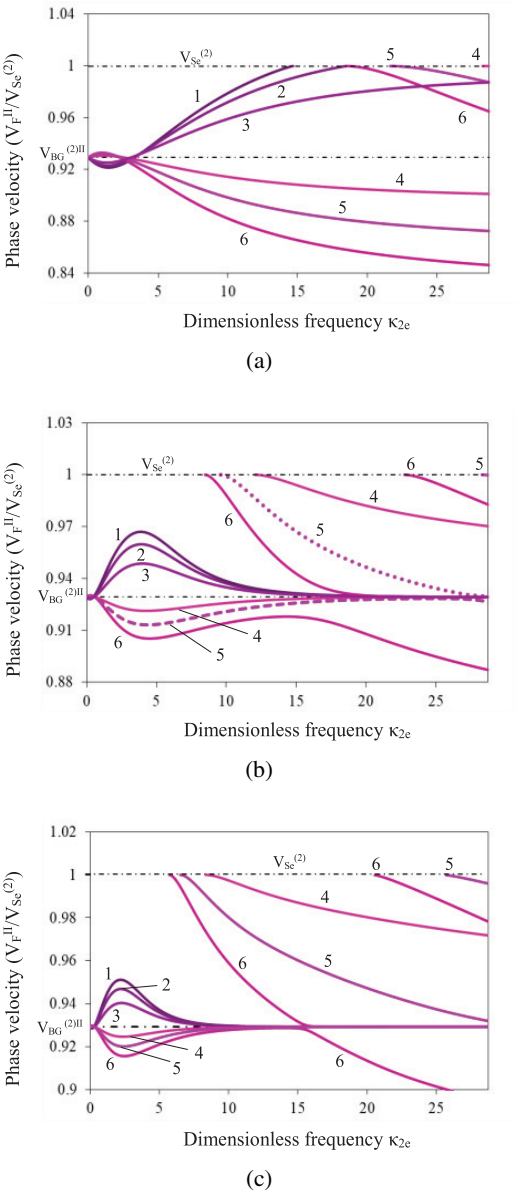

Fig. 4. Influence of the gradient coefficient of changes in the piezoelectric properties of the coating on the SAW velocity at different localization of inhomogeneity.

heterogeneity at the surface (Fig. 4(a)), in the middle (Fig. 4(b)) and at the base of the coating (Fig. 4(c)). The numbers 1–6 mark the curves corresponding to the values $\gamma_e = 2, 1.8, 1.5, 0.8, 0.6, 0.4$.

Figure 5 illustrates the effect of a change of dielectric modules ($\gamma_\varepsilon, \gamma_c = \gamma_e = 1$) on the SAW velocity when the heterogeneity is localized at the surface (Fig. 5(a)), in the middle (Fig. 5(b)) and at the base of the coating (Fig. 5(c)). Curves 1–6 correspond to the values $\gamma_\varepsilon = 2, 1.8, 1.5, 0.8, 0.6, 0.4$.

As follows from the figures, the location of the inhomogeneity significantly affects the characteristics of the SAW. The maximum effect on the SAW structure is exerted by a change of the modules at the coating surface. An increase of elastic modules leads to an increase of the velocity SAW and a reduction of the region of its existence. A decrease of the modules leads to a decrease of the velocity and the appearance of second SAW modes (Fig. 3). Piezoelectric modules have a similar effect on the SAW velocities, with the exception of the low frequency range. In this range, an increase of the modules leads to a decrease of the SAW velocity, and a decrease of the modules leads to an increase of the SAW velocity (Fig. 4).

A similar effect on the SAW velocity has dielectric modules. Their increase leads to a reduction, and a decrease

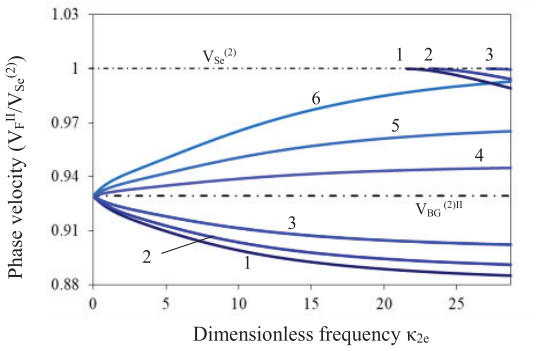

(a)

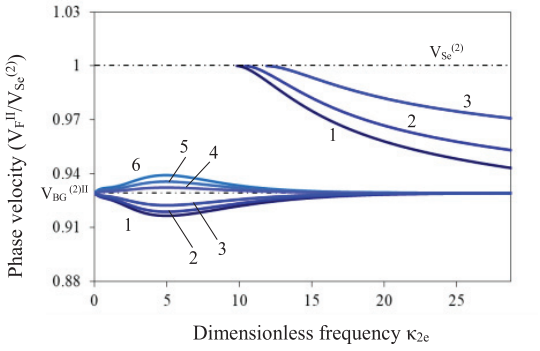

(b)

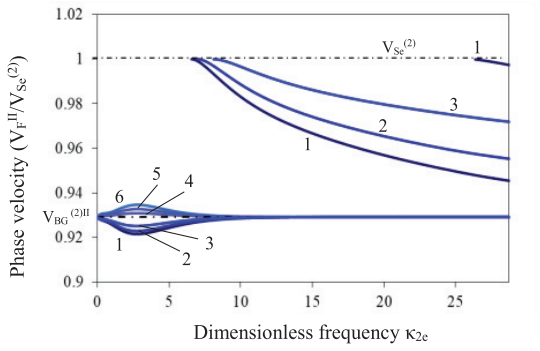

(c)

Fig. 5. Influence of the gradient coefficient of changes in the dielectric properties of the coating on the SAW velocity at different localization of inhomogeneity.

to increase of the SAW velocity (Fig. 5). The location of the heterogeneity in the middle or at the base of the coating qualitatively changes the structure of the SAW. It can be seen from the figures that the maximum range of velocity variation is achieved when the heterogeneity is localized at the coating surface. The moving of the inhomogeneity to the base of the coating qualitatively changes the structure of the surface wave field. The maximum effect on SAW velocity (Fig. 3) is exerted by the elastic modules of the coating. Piezoelectric coating modules have less impact. In the low-frequency region, an increase in the modules leads to a decrease in the SAW velocity, a decrease in the values of piezoelectric

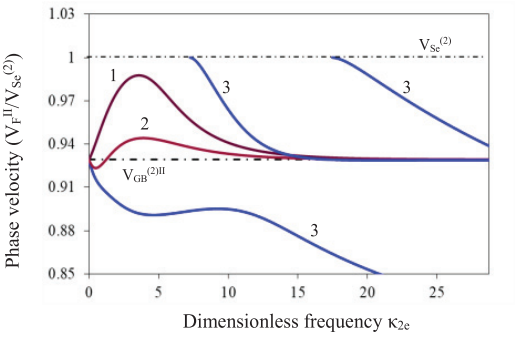

Fig. 6. SAW velocity for structures coated with materials with various combinations of gradient ratios.

modules leads to an increase in the SAW velocity. The situation changes with increasing frequency (Fig. 4). A decrease of dielectric modules leads to an increase of the SAW velocity, an increase of modules leads to a decrease of the velocity and the appearance of second SAW modes (Fig. 5). In addition, in the case of surface localization of inhomogeneity, an increase of both elastic and piezoelectric modules leads to an increase of the velocity and a limitation of the frequency range of the existence of SAW. In the first case, the frequency range is significantly less. A decrease of the values of these parameters leads to a decrease of the velocity and the appearance of second modes at high frequencies (Figs. 3(a) and 4(a)). In the case $\gamma_{c,e} < 1$, there are two modes of SAW. When the inhomogeneity moves to the base of the coating, the deviation of the velocity of the first SAW mode from the $V_{BG}^{(2)II}$ (the velocity of the Bluestein–Gulyaev wave) and the value of the frequency of occurrence of the second mode decreases and depends on the gradient coefficients of the change in properties and the area of the inhomogeneity localization. Figure 6 shows plots of SAW velocity for a coating structure m_1/m_2 (curve 1), m_1/m_3 (curve 2), and m_1/m_4 (curve 3). Inclusion materials m_2 and m_3 are rigid materials with a combination of gradient coefficients, respectively $\gamma_c = 1.5, \gamma_e = 2, \gamma_\varepsilon = 0.8$ and $\gamma_c = 0.8, \gamma_e = 2\gamma_\varepsilon = 2$. Soft material m_4 has gradient coefficients $\gamma_c = 0.6, \gamma_e = 1.5, \gamma_\varepsilon = 4$. The heterogeneity of the change of properties is localized in the middle of the coating.

As follows from Figs. 6, 3(b), 4(b) and 5(b), the nature of the change in the SAW velocity is determined by the choice of materials for the inclusion, coating and substrate, the gradient of inhomogeneity and its location over the thickness of the coating. The influence of various gradient coefficients of changes in material parameters on the SAW velocity can be either enhanced or weakened by the choice of a certain combination of materials. In the m_1/m_3 coating, greatest influence on the first mode has γ_c; the combination of γ_c and γ_ε influences on the frequency of the second mode and the character of behavior of its velocity.

Figure 7 shows the influence of the coefficients γ_c and γ_e for different localization of the inclusion in the coating on the SAW velocity in "open case". In Fig. 7(a) curves 1 and 2

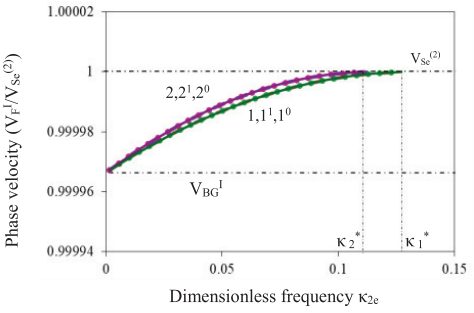

(a)

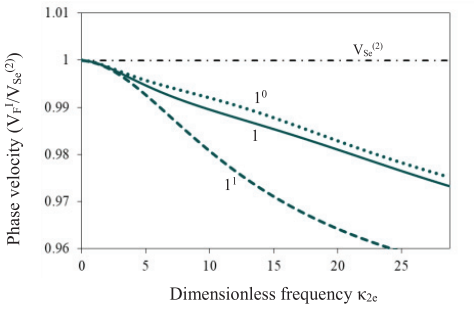

(b)

Fig. 7. Influence of the gradient coefficients γ_c and γ_e of the coating on the SAW velocity at different localization of the heterogeneity.

correspond to the values $\gamma_c = 1.5$, $\gamma_e = \gamma_\varepsilon = 1$ and $\gamma_e = 1.5$, $\gamma_c = \gamma_\varepsilon = 1$, in Fig. 7(b) curves 1 correspond to the values $\gamma_c = 0.8, \gamma_e = \gamma_\varepsilon = 1$. The superscripts 0, 1 mark the localization of the heterogeneity in accordance with Fig. 2.

The analysis showed that for $\gamma_c > 1$ and $\gamma_e > 1$, the SAW exists in a limited frequency range. The location of the inhomogeneity within the coating does not affect the velocity (Fig. 7 (a)). For $\gamma_c < 1$ and $\gamma_e < 1$, the SAW exists at any frequency.

4.2. *Determination of the initial strain state of the coating*

The initial stress state of the coating in the Lagrangian coordinate system is determined by the Kirchhoff stress tensor **P**, the material form of the electric induction vector **d**, and the Piola–Maxwell electric stress tensor **m**. Their components in the Cartesian coordinate system for materials of class 3m have the form:[21,26]

$$\begin{aligned}
P_{11} &= c_{11}^{(1)}S_{11} + c_{12}^{(1)}S_{22} + c_{13}^{(1)}S_{33} \\
&\quad + e_{22}^{(1)}W_2^0 - e_{31}^{(1)}W_3^0 + m_{11}, \\
P_{22} &= c_{12}^{(1)}S_{11} + c_{11}^{(1)}S_{22} + c_{13}^{(1)}S_{33} \\
&\quad - e_{22}^{(1)}W_2^0 - e_{31}^{(1)}W_3^0 + m_{22}, \\
P_{33} &= c_{13}^{(1)}S_{11} + c_{13}^{(1)}S_{22} + c_{33}^{(1)}S_{33} - e_{33}^{(1)}W_3^0 + m_{33}, \\
d_1 &= \varepsilon_{11}^{(1)}W_1^0 + de_1, \\
d_2^{(1)} &= -e_{22}^{(1)}S_{11} + e_{22}^{(1)}S_{22} + \varepsilon_{11}^{(1)}W_2^0 + de_2, \\
d_3 &= e_{31}^{(1)}S_{11} + e_{31}^{(1)}S_{22} + e_{33}^{(1)}S_{33} + \varepsilon_{33}^{(1)}W_3^0 + de_3,
\end{aligned}$$

$S_{ii} = \frac{1}{2}(\nu_k^2 - 1)$-components of the strain tensor, W_k^0-components of the electric field intensity vector

$$\begin{aligned}
m_{11} &= \varepsilon_0 \frac{\nu_2\nu_3}{2}((W_1^0\nu_1^{-1})^2 - (W_2^0\nu_2^{-1})^2 - (W_3^0\nu_3^{-1})^2), \\
m_{22} &= \varepsilon_0 \frac{\nu_1\nu_3}{2}((W_1^0\nu_1^{-1})^2 - (W_1^0\nu_1^{-1})^2 - (W_1^0\nu_1^{-1})^2), \\
m_{33} &= \varepsilon_0 \frac{\nu_1\nu_2}{2}((W_1^0\nu_1^{-1})^2 - (W_1^0\nu_1^{-1})^2 - (W_1^0\nu_1^{-1})^2), \\
de_k &= \varepsilon_0 \frac{\nu_1\nu_2\nu_3}{\nu_k^2} W_k^0
\end{aligned}$$

In this paper, the following types of IDS coating are considered:

$$\begin{aligned}
&1x_1 : P_{11} = P, \quad P_{22} = P_{33} = 0, \quad W = \{0, 0, 0\}, \\
&2E_{23}^{++} : P_{11} = P_{22} = P_{33} = 0, \quad W = \{0, W_2^0, W_3^0\}, \\
&1x_1E_{23}^{++} : P_{11} = P, \quad P_{22} = P_{33} = 0, \quad W = \{0, W_2^0, W_3^0\}.
\end{aligned}$$

***Note*:** the electric field intensity W_2^0 is clearly not present in the coefficients $\theta_{ikl}^{(1)}$ involved in the representation of equations of motion (14) and boundary conditions (17), (18), (20), though, in contrast to structures with piezoceramic coatings based on PZT,[26] influence on IDS coating.

4.3. *Influence of initial mechanical impacts and electrical field on SAW velocities*

Figures 8(a)–8(c) show the effect of the initial mechanical action and external electric field on the SAW velocity for structures with an inhomogeneous coating of materials m_1/m_2 (Fig. 8(a)), m_1/m_3 (Fig. 8(b)) and m_1/m_4 (Fig. 8(c)).

A short case is considered (***problem II***), the heterogeneity of properties is localized in the middle of the coating. Dashed and dotted lines 1 and 2 correspond to the $1x_1$ IDS coating caused by the action of mechanical stresses with deformations $\nu_1 = 1.03$ and 0.97. Curves 3 and 4 correspond to the IDS induced in the coating by the combined action of mechanical stresses and an electric field $1x_1E_{23}^{++}$ ($\nu_1 = 0.97, W_2^0 = W_3^0 = 0.01$) and the action of an electric field $2E_{23}^{++}$ in the absence of mechanical stresses. The number 0 marks the SAW velocity curves for structures with an inhomogeneous coating in the NS. The intensity of the initial electric field $W_i^0 = 0.01$ in dimensional units corresponds to $1 \cdot 10^8$ V/m.

It follows from the figures that the presence of uniaxial mechanical tension (curves 1) leads to an increase of the SAW velocity for the considered combinations of coating materials, the presence of uniaxial mechanical compression (curves 2) leads to a decrease of the velocity.

In contrast to the PZT-based coatings,[26] an inhomogeneous structure of piezoceramic coating based on $LiNbO_3$ resistant to the electric field (curves 3 and 4): high intensity field effect leads to slight SAW velocity changes. A change in the direction of the electric field intensity with a combined

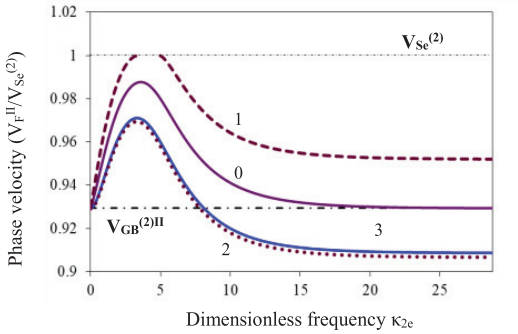

(a)

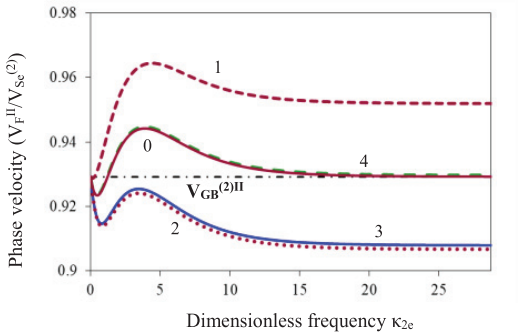

(b)

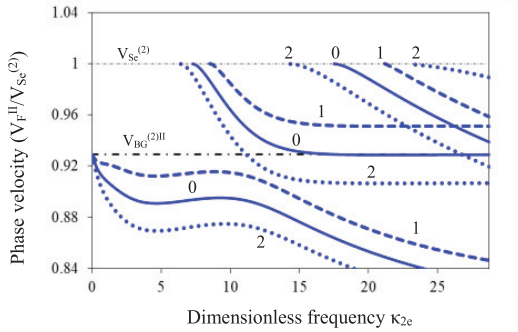

(c)

Fig. 8. The combination of coating materials: m_1/m_2 - (a), m_1/m_3 - (b); m_1/m_4 - (c). A short case is considered (Problem II).

mechanical impact and electrical field can enhance or weaken the effect of mechanical stresses.

5. Conclusion

Within the framework of the linearized theory of electroelasticity, a model of a piezoelectric structure with a prestressed functionally graded coating made of piezoceramics of a trigonal system with a symmetry class 3m in the NS is considered. Ferroelectric $LiNbO_3$ was used as the main material of the structure. It is assumed that the initially deformed state (IDS) of the coating material is uniform, induced by the action of initial mechanical stresses and an electric field, and the properties of the coating change continuously in a non-monotonous manner over the thickness. The properties of the coating continuously change in thickness. Linearized constitutive relations and equations of motion of the electroelastic medium are used, which make it possible to take into account the effect of the initial deformation on both the elastic and piezoelectric and dielectric properties of the coating material. The model takes into account both joint and separate effects of mechanical influences and an electric field. Problems of the propagation of SH-waves from a remote source for structures with an inhomogeneous prestressed coating in a "short" and "open" case are considered. The analysis of the features of the structure of the SAW with different structures of the coating and various types of IDS was carried out on the basis of solving boundary value problems of the theory of electroelasticity for media with inhomogeneous coating, using the numerical–analytical method for constructing the Green's functions of the medium and analyzing its dispersion properties. For heterogeneous coatings in the NS, the influence of the gradient coefficients of changes in the elastic piezoelectric and dielectric properties of the coating material on the features of the propagation of SAW is investigated. The transformation of the surface wave field is shown depending on the location of the inhomogeneity inside the coating. The regularities of the influence of IDS on the SAW rate for coatings with inclusions from various materials (m_1, m_2, m_3, m_4) have been established. A significant change of the SAW velocity under a purely mechanical initial action is shown. In the case of m_1/m_2 coating, it leads to the disappearance of the SAW in a certain frequency range. With a combined mechanical and electrical impact, due to a change in the direction of the electric field intensity, it is possible to enhance or weaken the effect of mechanical stresses. This phenomenon can have a large effect in the vicinity of critical frequencies (frequencies of the disappearance of SAW or the generation of new surface waves).

Acknowledgments

This work was performed with a financial support of the Ministry of Science and Higher Education of the Russian Federation (project 01201354242) and Russian Foundation of Basic Research (projects 19-08-01051, 19-01-00719).

References

[1]W. P. Mason, *Physical Acoustics and the Properties of Solids* (Princeton, N.J., Van Nostrand, 1958).
[2]E. Dieulesaint and D. Royer, *Ondes Elastiques Dans Les Solides: Application au traitement du signal* (Masson, Paris, 1974)
[3]H. Matthews, *Surface Wave Filters: Design, Construction and Use* (Wiley, New York, 1977).
[4]J. Bernhard and J. V. Michael, Properties of Love waves: Applications in sensors, *Smart Mater. Struct.* **6**, 668 (1997).
[5]S. V. Biryukov, Y. V. Gulyaev, V. V. Krylov and V. P. Plessky, *Surface Acoustic Waves in Inhomogeneous Media* (Springer-Verlag, New York, 1995).

[6]F. Jin, Z. Wang and T. Wang, The Bleustein–Gulyaev (B–G) wave in a piezoelectric layered half-space, *Int. J. Eng. Sci.* **39**, 1271 (2001).
[7]X. Han, G. R. Liu, K. Y. Lam and T. Ohyoshi, A quadratic layer element for analyzing stress waves in FGMs and its application in material characterization, *J. Sound Vib.* **236**(2), 307 (2000).
[8]X. Y. Li, Z. K. Wang and S. H. Huang, Love waves in functionally graded piezoelectric materials, *Int. J. Solids Struct.* **41**, 7309 (2004).
[9]X. Cao, F. Jin and I. Jeon, Calculation of propagation properties of Lamb waves in a functionally graded material (FGM) plate by power series technique, *NDT&E Int.* **44**, 84 (2011).
[10]B. Collet, M. Destrade and G. A. Maugin, Bleustein–Gulyaev waves in some functionally graded materials, *Eur. J. Mech. A Solids* **25**, 695 (2006).
[11]J. Du, X. Jin, J. Wang and K. Xian, Love wave propagation in functionally graded piezoelectric material layer, *Ultrasonics* **46**(1), 13 (2007).
[12]X. Cao, F. Jin, I. Jeon and T. J. Lu, Propagation of Love waves in a functionally graded piezoelectric material (FGPM) layered composite system, *Int. J. Solids Struct.* **46**, 4123 (2009).
[13]Z.-H. Qian, F. Jin and S. Hirose, Dispersion characteristics of transverse surface waves in piezoelectric coupled solid media with hard metal interlayer, *Ultrasonics* **51**, 853 (2011).
[14]P. Li, F. Jin and T.-J. Lu, A three-layer structure model for the effect of a soft middle layer on Love waves propagating in layered piezoelectric systems, *Acta Mech. Sin.* **28**(4), 1087 (2012).
[15]Z. N. Danoyan and G. T. Piliposian, Surface electro-elastic shear horizontal waves in a layered structure with a piezoelectric substrate and a hard dielectric layer, *Int. J. Solids Struct.* **45**, 431 (2008).
[16]M. Pluta, M. von Buttlar, A. Habib *et al.*, Modeling of Coulomb coupling and acoustic wave propagation in $LiNbO_3$, *Ultrasonics* **48**(6–7), 583 (2008).
[17]A. Y. Borisevich and P. K. Davies, Crystalline structure and dielectric properties of $Li_{(1+x-y)}Nb_{(1-x-3y)}Ti_{(x+4y)}O_{(3)}$ M-phase solid solutions, *J. Am. Ceram. Soc.* **85**(3), 573 (2002).
[18]O. Yu. Kravchenko, L. A. Reznichenko, L. A. Shilkina, O. N. Razumovskaya, S. I. Dudkina, G. G. Gadzhiev, S. N. Kallaev and Z. M. Omarov, Properties of $Na_{0.875}Li_{0.125}NbO_3$ ceramics, *Inorg. Mater.* **44**(10), 1135 (2008).
[19]O. Yu. Kravchenko, L. A. Reznichenko and D. S. Fomenko, Dielectric properties of $Na_{1-x}K_xNbO_3$ and $Na_{1-x}Li_xNbO_3$ ceramics, *Inorg. Mater.* **47**(5), 561 (2011).
[20]M. N. Palatnikov, O. B. Shcherbina, V. V. Efremov, N. V. Sidorov and A. N. Salak, Microstructure and young's modulus of high-pressure $Li_xNa_{1-x}Ta_yNb_{1-y}O_3$ ceramics, *Inorg. Mater.* **47**(6), 686 (2011).
[21]V. V. Kalinchuk and T. I. Belyankova, *Dynamic Contact Problems for Prestressed Electroelastic Media* (Fizmatlit, Moscow, 2006).
[22]T. I. Belyankova and V. V. Kalinchuk, *Dynamics of a Surface of Inhomogeneous Media* (Fizmatlit, Moscow, 2009).
[23]T. I. Belyankova, V. V. Kalinchuk and O. M. Tukodova, Peculiarities of the surface SH – waves propagation in the weakly in homogeneous pre-stressed piezoelectric structures, in *Advanced Materials, Springer Proceedings in Physics* Vol. 175 (Springer, 2016), p. 143.
[24]T. I. Belyankova, E. I. Vorovich, V. V. Kalinchuk and O. M. Tukodova, Peculiarities of surface acoustic waves, propagation in structures with functionally graded piezoelectric materials, coating from different ceramics on the basis of PZT, *J. Adv. Dielectr.* **10**(1–2), 2060017 (2020).
[25]T. I. Belyankova and V. V. Kalinchuk, Shear horizontal waves in piezoelectric structures with a functionally graded coating, *Mech. Adv. Mater. Struct.* **28**(5), 486 (2021).
[26]T. I. Belyankova and V. V. Kalinchuk, Influence of an electrostatic field on SAW in prestressed ferroelectric heterostructures, *Mech. Solids* **55**, 844 (2020).
[27]T. Yamada, N. Niizeki and H. Toyoda, Piezoelectric and elastic properties of lithium niobate single crystals, *J. Appl. Phys.* **6**(5), 151 (1967).
[28]A. W. Warner, M. Onoe and G. A. Coquin, Determination of Elastic and Piezoelectric Constants for Crystals in Class (3m), *J. Acoust. Soc. Am.* **42**(6), 1223 (1967).